TRENDS IN SCIENCES 2025; 22(7): 9978
https://doi.org/10.48048/tis.2025.9978 RESEARCH ARTICLE

Study of The Encapsulation of Local Anaesthetic Drugs in B-Cyclodextrin in Solid and Liquid States

Fatima Zohra Chater[1], Youcef Bouhadda[1,*], Teffaha Fergoug[1], FatimaYssaad[1], Mahmoud Belalia[2], Rachida Aribi[1], Cherifa Zelmat[1,3] and Meriem Dadouch[1,4]

[1]Laboratory of Physical Chemistry of Macromolecules and Biological Interfaces, University Mustapha Stambouli of Mascara, Mascara 29000, Algeria
[2]Laboratory SEA2M, Abdelhamid Ibn Badis University, Mostaganem 27000, Algeria
[3]Departement of Chemistry, University Djillali Liabes of Sidi Bel Abbes, Sidi Bel Abbes 22000, Algeria
[4]Departement of Pharmacy, Faculty of Medicine, University Djillali Liabes of Sidi Bel Abbes, Sidi Bel Abbes 22000, Algeria

([*]Corresponding author's e-mail: y.bouhadda@univ-mascara.dz)

Received: 11 February 2025, Revised: 27 March 2025, Accepted: 3 April 2025, Published: 30 May 2025

Abstract

Local anesthetics (LAs) are widely used in medical practice, but their efficacy and stability can be improved through molecular complexation with cyclodextrins (CDs). Beta-cyclodextrin (β-CD), in particular, is known for its ability to form inclusion complexes, enhancing drug solubility and bioavailability. This study explores the molecular interactions between β-CD and three Las - tetracaine (TC), tetracaine hydrochloride (TC·HCl), and procaine hydrochloride (PC·HCl) - using complementary analytical techniques. Since these complexed drugs can be delivered either as liquid-like injections or as solid-like paste and to gain a thorough understanding of the complexation behavior, analyses in both liquid-state (aqueous solution) and solid-state were conducted. Techniques such as ultraviolet-visible spectroscopy (UV-Vis) and isothermal titration calorimetry (ITC) in aqueous solution and differential scanning calorimetry (DSC) and Fourier transform infrared spectroscopy (FT-IR) in solid state were used. The UV-Vis and ITC methods gave comparable results regarding the complex formation constants for TC, HCl and PC, HCl complexes but seemed to diverge in the case of basic tetracaine. The ITC data indicated that the 1 site model fits well for TC, HCl/β-CD complex and moderately for PC, HCl/β-CD complex but it was not adapted to the basic tetracaine. The binding process of β-CD with hydrochloride type drugs in liquid state is exothermic, enthalpy controlled and entropy driven since the values of the corresponding binding enthalpies ΔH are negative, fairly lower than of TΔS terms at 298.15 K The solid state characterization of the LA/β-CD complexes by DSC and IR methods showed that the complexation of the hydrochloride LAs into β-CD cavity occurred during both physical mixture and kneading preparations. The IR spectra analysis suggested that the inclusion of hydrochloride type drugs into CD cavity is not exclusively hydrophobic effect driven which probably explains the divergent behavior observed from ITC experiments for the basic tetracaine. IR results supported and completed the conclusions drawn from liquid state investigation.

Keywords: Cyclodextrin, Anaesthetic drug, UV-Vis spectrophotometry, Procaine hydrochloride, Molecular encapsulation, Differential scanning calorimetry, Isothermal titration calorimetry

Introduction

Local anaesthetics (LAs) are drugs that inhibit pain perception by interacting directly with voltage-gated channels [1]. These channels are a subtype of integral transmembrane proteins, and the binding sites for the drugs can be located on any domains of these proteins (extracellular loop, transmembrane, or cytoplasmic domains) [2]. It is proposed that upon reaching the appropriate domain, the drugs bind to specific receptors, leading to a conformational change in the binding site of the protein, which in turn stops the initiation and transmission of nerve impulses [3]. This ability is possible thanks to the chemical structure of these drug molecules which are structured into three parts. The 1st one constituted by an aryl group is of hydrophobic nature whereas the 2nd one is hydrophilic since it contains a tertiary ammonium group. These 2 groups give LA molecules an amphiphilic character and enable LA molecules to behave in aqueous solution such as surfactants by adsorbing preferentially at interfaces and further above a critical concentration forming micelles. Between these 2 antagonist parts stands the so-called intermediate part which can bear either an ester or amide chemical function with which the anaesthetic properties are associated partly. It is well established that in aqueous solution, the ammonium group switches into amine one when the pH increases which permits to LA molecules to diffuse through non polar media like nervous cell membranes. While the neutral form of the drugs facilitates the movement from the extracellular space across the lipid bilayer into the cytoplasm, the charged form exerts the blocking effect. Although a direct pathway for quaternary drug forms from the exterior is seldom proposed, it is not entirely ruled out, as reports concerning cardiac sodium channels show [1-3]. Moreover, the ability to proton transfer from the ammonium atom classifies local anesthetics (LAs) as weak acids. Consequently, at a given pH, their acidic form can coexist with their conjugate base in a state of chemical equilibrium. It is also suggested that the interplay between their hydrophilic/lipophilic characteristics and their acid/base properties influences their potency to some degree [4]. In the formulation of anesthetic drugs, a significant challenge arises from their poor solubility in water, particularly in the case of the basic unprotonated form, while the acidic form exhibits slightly better solubility. Therefore, it is common to encounter anaesthetic drugs formulated as hydrochlorides or combined with specific solubilizing agents. One of the most frequently utilized additives to enhance the solubility of these drugs in water are cyclodextrins [5,6]. Of course, other advanced drug delivery systems are employed to improve the solubility, stability, and bioavailability of anesthetic drugs. One can cite liposomes, Polymeric nanoparticles made of PLGA (poly(lactic-co-glycolic acid)), Micelles, dendrimers, and Hydrogels as picked examples [7-10]. However, cyclodextrins remain the best option since they are biodegradable, non-toxic, and water-soluble, capable of encapsulating various water-insoluble therapeutic compounds within their hydrophobic cavities. The process of complexation itself represents a chemical equilibrium that must be considered with the others equilibria, such as acid/base and micelle/monomer equilibria. When concentrations are well below the threshold for micelle formation, only the processes of complexation and deprotonation coexist. Complexation is likely to be facilitated when the basic form of the local anaesthetic is present, as it is assumed that hydrophobic interactions primarily drive the inclusion of such drugs within the cyclodextrin cavity, thereby enhancing the formulation [11,12].

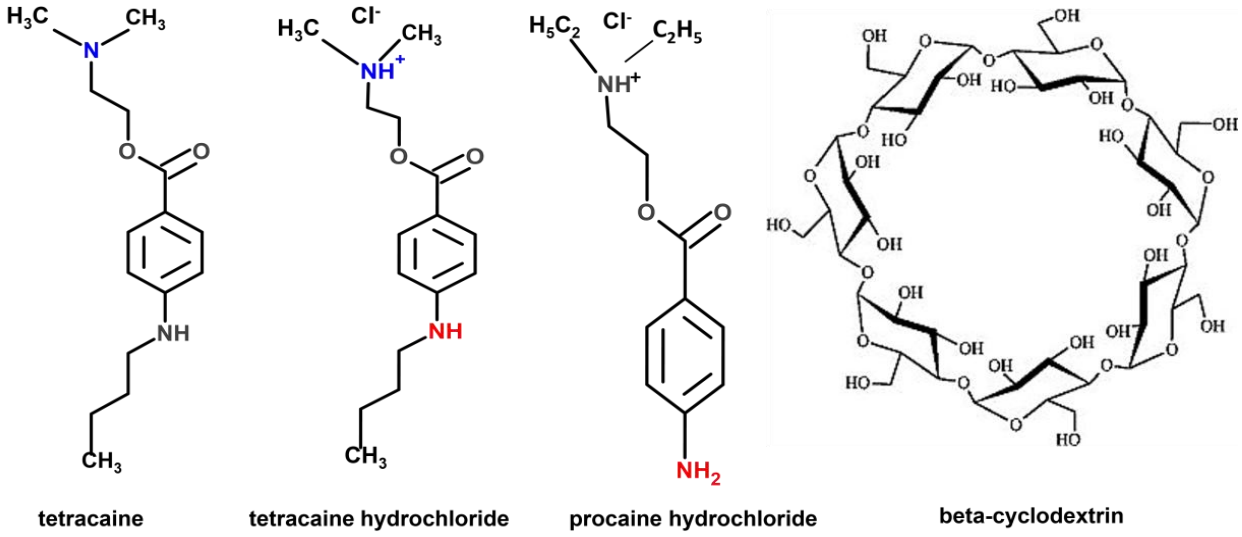

Figure 1 Chemical structures of: (a) Tetracaine, tetracaine hydrochloride, procaine hydrochloride and (b) Beta-cyclodextrin (β-CD).

So, it is interesting to explore the contribution of acid/base species and lipophlic/hydrophilic parts on the complexation process and hence on the success of drug formulation. For this, we selected three drugs belonging to the same group of LAs: tetracaine (TC) and tetracaine hydrochloride (TC, HCl) beside procaine hydrochloride (PC, HCl). These drugs have been chosen as model β-cyclodextrin ligands to explore β-CD-ligand interactions using DSC, IR, UV-vis and ITC. It is worth to remind that basic tetracaine TC, tetracaine hydrochloride TC, HCl and procaine hydrochloride PC, HCl belong to the aminoester family of LAs, an important class of nociceptive agents [3], and are commonly used in local topical anaesthesia in dentistry and ophthalmology [13-17]. They are also components of some anaesthetic gels used in veterinary practices [18-20]. β-cyclodextrin (β-CD) is one of the most important host compounds in pharmaceutical industry and represents one of the most used excipient [21-24]. The β-CD is a cage-shaped molecule with a cyclic oligosaccharide containing 7 D (+) glucopyranose units (**Figure 1(b)**), which confer it a hydrophilic exterior and hydrophobic internal cavity that enable it to complex with a non-polar part of a guest molecule [25-28].

TC and TC, HCl have almost similar chemical structures (**Figure 1(a)**) but differ by the presence of proton on the nitrogen atom on TC, HCl which must induce a conformational difference that is very sensitive from inclusion process point of view. In front of this, TC, HCl and PC, HCl couple also have close chemical structures but differ on the hydrophobic parts. The aryl-group carries a butyl fragment in TC, HCl, whereas only a primary amine fragment is available in PC, HCl (**Figure 1(a)**). The goal of our study is to examine the effect of these particular differences on the host-guest interaction in the liquid phase and the solid phase. This is an interesting approach since the majority of the investigations on host-guest interaction are performed exclusively for the liquid state or the solid state.

Materials and methods

Materials

4-(Butylamino) benzoic acid 2- (dimethylamino) ethyl ester monohydrochloride, commonly named tetracaine hydrochloride (TC, HCl) and its basic form (TC), procaine hydrochloride for 4-aminobenzoic acid, 2(diethylamino) ethyl ester (PC, HCl) and β-cyclodextrin (β-CD) with 99 % purity or greater, were ~~also~~ purchased from Sigma and used without further purification. All the solutions were freshly prepared with deionized water with conductivity lower than 0.7 μS /cm and pH around 7. The homogeneity of the initial solutions was ensured by ultrasonic bath. In the case of CD solutions, the sonication process lasted more than 24 h, while only 1 h was sufficient for drug solutions.

Preparation of the samples

Physical mixtures

The physical mixture (PM) made of the drug (LAs) and cyclodextrin β-CD in a molar ratio of (1:1) was obtained by mixing the corresponding pure compounds with a spatula until the mixture looks homogenous with a moderate grinding if necessary. A portion of the prepared PM sample was further subjected to a rigorous manual grinding in a glass mortar with a pestle for 30 min to produce a finer powdered sample PM_f.

Kneading method (KN)

The kneading preparation was adapted from Prabu *et al.* [29] study, it consists of mixing an equi-molar amounts (1:1) of (LAs) and β-CD in a mortar and grinding them with a pestle while adding gradually small amounts of deionized water until suitable consistency is achieved. The final product was dried at 45 °C for 48 h and then further ground to a fine powder.

Apparatus and methods

Ultraviolet-visible (UV-vis) spectroscopy

All UV-Vis spectra were recorded using a Specord 200 plus double-beam UV-Vis spectrophotometer (Germany), with wavelength range of 190 to 400 and 1 nm intervals at 25 °C. The temperature was kept constant with a thermostated cell. In the experiments with the drug/water binary systems, the LAs concentration was 5.10^{-5} M but for the β-CD /LAs/water ternary systems the β-CD concentration was varied from 0.01 M to 1 μM and the drug concentration was fixed to 50 μM.

Isothermal titration calorimetry (ITC)

ITC experiments were performed using a Nano ITC low volume apparatus (TA instruments) at ambient temperature (temperature of 298.15 ± 0.5 K). A calibration of the calorimeter was carried out electrically and the $CaCl_2$-EDTA titration was performed to ensure that the apparatus was operating correctly. The results (n-stoichiometry, K, ΔH) were compared with those obtained for the same samples (a test kit: A standardized set of reagents and acceptable values for (n-stoichiometry, K, ΔH) provided by the manufacturer (TA Instruments) to validate the performance of the Nano ITC calorimeter). Prior to the titration all samples were degassed with a TA degasser for 1 h. The sample cell was filled with 280 μL of β-CD solution and the titrant syringe was filled with 40 μL of LA solution. Whereas, the reference cell was filled with deionized and degassed water. Incremental ITC with 25 injections of 10 μL each (except 2 μL for the 1st injection) were performed at a rate of 0.5 μL per second, spacing 150 s to allow a complete return to the baseline. The following settings were used: Stirring speed 200 rpm, reference power 5 μCal per second, feedback mode/gain set to high, initial delay 200 s and filter period 2 s. The same setting parameters were also used for β-CD and LA dilution experiments. The heats of dilution of the LA and the β-CD were small compared with the heat of binding and were subtracted from the experimental titration results. The volume change in the mixing cell due to the injection of the LA solution was corrected automatically by the Nanoanlyse software v.3.10.0 provided by the manufacturer (TA Instruments). The data of the 1st injection were discarded due to diffusion between the syringe and the sample cell solution. The registered data were analyzed based of the model of a single set of identical sites. This model assumes a single type of binding site and a 1:1 stoichiometry between the ligand X and the macromolecule M. The reaction can be written as:

$$M+nX \rightleftharpoons MXn \quad (1)$$

and the equilibrium constant (K) defined as:

$$K = [MXn]/[M][X]^n \quad (2)$$

where, [MXn], [M] and [X] stand for concentration of the Host-ligand complex, concentration of Host macromolecule and concentration of the ligand respectively.

Given the expression of equilibrium constant K for one site model, one can write:

$$K = \frac{\Theta}{(1-\Theta)[X]} \quad (3)$$

$$\text{with } X_t = [X] + n\Theta \mathrm{M_t} \quad (4)$$

where, Mt and [M] are bulk and free concentration of macromolecule; Xt and [X] are bulk and free concentration of ligand, Θ is the fractional saturation term (Θ = [MXn]/([M]+[MXn])) and n the number of sites or (order or stoechiometry of the reaction of binding). Combining these 2 equations above gives;

$$\Theta^2 - \Theta\left[1 + \frac{X_t}{nM_t} + \frac{1}{nKM_t}\right] + \frac{X_t}{nM_t} = 0 \quad (5)$$

So the total heat content Q of the solution contained in Vo (active cell volume) at fractional saturation Θ is:

$$Q = n\Theta M_t \Delta H V_0 \quad (6)$$

where ΔH is the molar heat of ligand binding. Solving the quadratic equation for Θ and then substituting this into the above equation gives:

$$Q = \frac{nM_t\Delta HV_0}{2}\left[1 + \frac{X_t}{nM_t} + \frac{1}{nKM_t} - \sqrt{\left(1 + \frac{X_t}{nM_t} + \frac{1}{nKM_t}\right)^2 - \frac{4X_t}{nM_t}}\right] \quad (7)$$

The value of Q above can be calculated (for any designated values of n, K, and ΔH) at the end of the ith injection and designated Q(i).

Based on the values of equilibrium constant (K) and enthalpy of complex formation (ΔH), the Gibbs energy of complex formation (ΔG) and the entropy of complex formation (ΔS) can been calculated, for all the investigated systems, from the following equations:

$$\ln K = -\frac{\Delta G}{RT} \quad (8)$$

$$\Delta G = \Delta H - T\Delta S \quad (9)$$

where T is the temperature (K) and R is the gas constant (8.314 J/ mol K).

Differential scanning calorimetry (DSC)

DSC analyses of the samples were carried out using Differential Scanning Calorimeter (Shimadzu DSC-A60) for a temperature range of 25 to 200 °C with a heating rate of 10 °C min^{-1}. During the experiments, aluminum crucibles with about 2 mg of samples were used, under dynamic N_2 atmosphere (50 mL min^{-1}) and using an empty sealed pan as reference [33]. DSC-A60 calorimeter was calibrated with indium sample (mp 156.6 °C; ΔH_{fus} = 28.54 J/g).

Fourier transform infrared spectroscopy (FT-IR) analysis

All DSC samples were subjected to IR spectroscopy characterization. FT-IR spectral data of pure solid compounds and solid inclusion complexes were recorded at room temperature by Nicolet iS10 FT-IR Spectrometer covering the range of 4,500 - 500 cm^{-1}. The spectra were acquired with an average of 32 scans with spectral resolution of 2 cm^{-1} in attenuated total reflectance (ATR) mode using Diamond crystal and operating with the OMNIC software provided by the manufacturer.

Results and discussion

UV-VIS spectroscopy studies

UV-VIS spectroscopy was initially employed to investigate the host-guest interactions, to demonstrate the formation of the complex and to determine the stoichiometry and stability constant of the β-CD/LA complex. The absorption spectra of LAs in water, recorded at a temperature of 25 °C both in the absence and presence of β-CD, are showed in **Figure 2** where the arrow 1 to 8 on each series of spectra ((a) for TC/β-CD, (b) for TC,HCl/β-CD and (c) PC,HCl/β-CD) indicates the increasing concentration of the β-CD. The absorption maxima corresponding to the aminobenzoate chromophore were identified at 292, 293 and 295 nm wavelengths for TC, TC, HCl and PC, HCl aqueous solutions, respectively. The clear emergence of isosbestic points in the three spectra indicates the presence of a chemical equilibrium between the complexed and unbound drug molecules.

The combined observations of maximum wavelength shifts in both intensity (hyperchromic) and position (bathochromic) indicate that the formation of the complexes (TC/β-CD), (TC, HCl/β-CD), and (PC, HCl/β-CD) has indeed occurred for the three drug molecules. Considering that their concentrations remain constant throughout the experiments and that β-

CD does not absorb light at this wavelength range. Consequently, we can claim that a portion of LA molecules is likely encapsulated within the β-CD cavity. Additionally, the distinct features observed in each spectrum regarding wavelength and absorbance variations suggest that different complexation mechanisms may have occurred, despite the structural similarity of the chromophores present in these molecules.

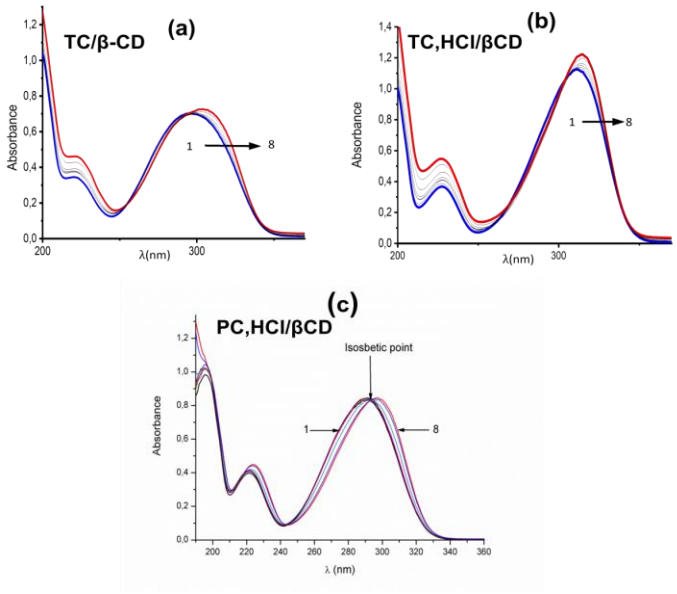

Figure 2 UV-Vis absorption spectra of the three LAs: (a) TC/β-CD, (b) TC,HCl/β-CD and (c) PC,HCl/β-CD.

The fitting of the variation of $\Delta\lambda = \lambda - \lambda_0$ and $\Delta A = A - A_0$ with β-cyclodextrin concentration were performed using the derived Eqs. (10) and (11) for 1:1 complex model [30-32].

$$\frac{\Delta A}{c} = \Delta\varepsilon \frac{K_{11}[CD]f}{1+K_{11}[CD]f} \quad (10)$$

$$\Delta\lambda = \Delta\lambda_{max}.\beta = \Delta\lambda_{max}.\frac{K_{11}[CD]f}{1+K_{11}[CD]f} \quad (11)$$

where (A and A_0) and (λ and λ_0) are respectively the absorbance and the maximum wavelength of the solutions in presence and in absence of CD. K_{11} and ($\Delta\lambda_{max}$, $\Delta\varepsilon$) represent the complexation constant and fitting parameters, respectively. These last expressions are derived from the assumptions that the change in absorbance (ΔA) during complexation is proportional to the concentration of the complex (MXn) and the molar absorptivity change upon complexation (Δϵ) and that the shift in wavelength (Δλ) is proportional to the fraction of bound guest molecules and the maximum possible shift at full saturation (Δλmax). Changes in ΔA for the mixture (TC,HCl/β-CD) or in Δλ for the mixtures (PC,HCl/ β-CD) and (TC/β-CD) against of β-CD concentration at T = 25 °C are shown on (**Figure 3**). The non-linear fitting of the data of the three curves applied to 1:1 stoichiometry model with Eqs. (1) and (2) enables the deduction the K_{11} complexation constants as illustrated in **Table 1**.

Table 1 Formation constant (K_{11}) values for β-CD/Las.

Complex	Formation constant, K_{11}
TC/β-CD	100.55
TC,HCl/β-CD	403.27
PC,HCl/β-CD	223.18

The obtained K_{11} values reflect a moderate affinity of β-CD for both TC, HCl and PC, HCl, which is suitable from a pharmacological point of view. On the contrary, a higher affinity between the drug and the β-CD is observed for TC, HCl which may lead to difficult delivery of the TC, HCl to the organism compared to the 2 other drugs. The higher affinity of β-CD to TC, HCl compared to TC may be attributed to the unavailability of free monomeric basic TC molecules in bulk solution at this concentration range and temperature since this basic form is known for its insolubility in water.

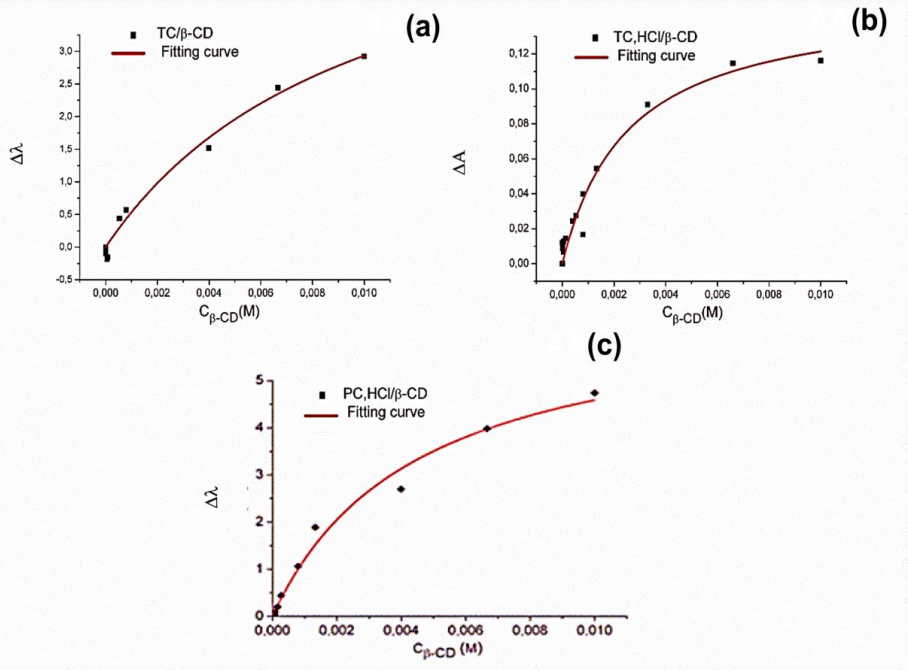

Figure 3 Variation of ΔA for (b) TC, HCl/β-CD, Δλ for (a) TC/β-CD and (c) PC, HCl/ β-CD systems as a function of β-CD concentration at T = 25 °C.

ITC measurements

ITC is well known as the most accurate method to determine the thermodynamic parameters for the ligand-CD interaction and to extract parameters such as stoichiometry (n) and binding constant (K). **Figure 4** shows both the calorimetric titration profiles and the corresponding reaction heats isotherms for the LA drugs binding to β-CD in aqueous solutions at temperature of 25 °C (298.15 ± 0.5 K and p = 0.1 MPa). **Table 2** summarizes the thermodynamic parameters calculated from ITC enthalpogram. In **(Figure 4)** it is obvious to note that different enthalpograms profiles are exhibited especially those of basic tetracaine TC. In fact, the basic tetracaine case shows an incomplete sigmoidal shape profile which leads to unexpected non realistic fitting parameters (inappropriate value for n = 0.1) and hence makes the data for the interaction of this drug with β-CD less accurate comparing with the 2 other guests. These results may reveal that the amount of free basic tetracaine molecules in the bulk solution is limited to induce host-guest interaction as suggested form UV-Vis data. For the 2 other hydrochlorides LAs, better profiles are obtained with negative ΔG ° values implying spontaneous processes that favor the binding interaction [34,35].

It can be seen from **Table 2** that the calculated ΔH^o for TC,HCl and PC,HCl systems are negative which means that the corresponding complexation processes are exothermic underlying the favourable non-covalent interactions between the host and the guest. In addition, the deduced standard formation entropies (ΔS°) are positive in all cases as usually reported for such molecules with a slight excess for PC,HCl complex. So, to compare the data for the 2 hydrochloride drugs, it is necessary to consider that the

strength of interaction depends on the width of the CD cavity, the volumes of penetrating part of the guest molecules and propensity of β-CD internal water molecules to leave the cavity.

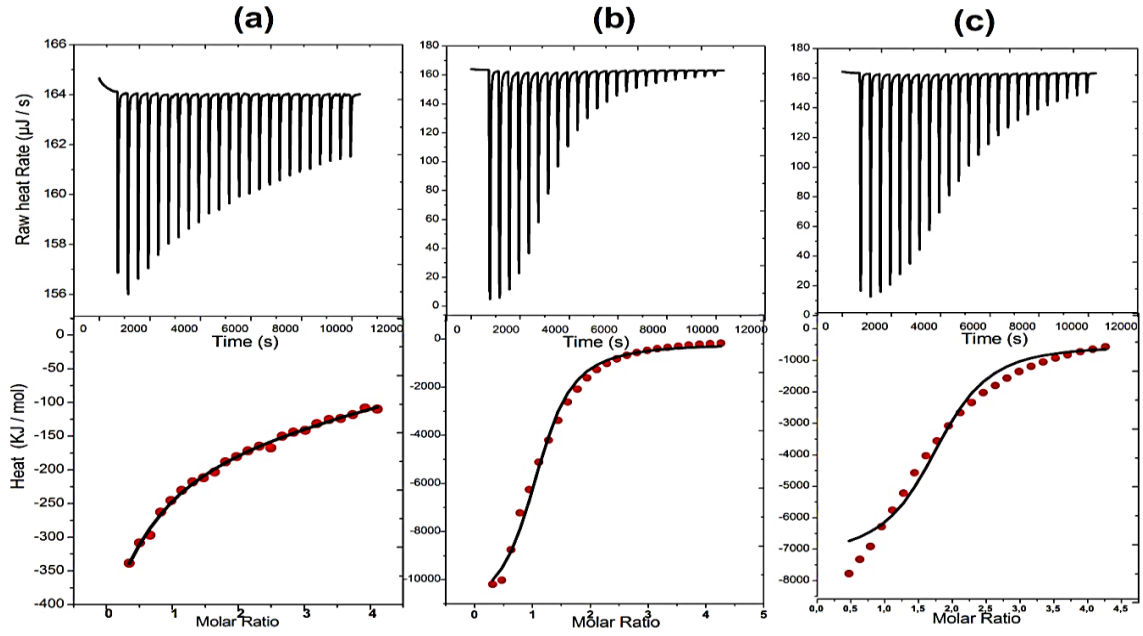

Figure 4 Calorimetric titration of LAs: (a) TC, (b) TC,HCl and (c) PC,HCl with the β-CD. Top: Raw data for 28 sequential injections (10 µL per injection) of β-CD solution into the LA solution. Bottom: Reaction heat isotherms obtained from the integration of the calorimetric curves. The line was drawn with the calculated parameters given in **Table 2**.

Furthermore, the general picture of hydrophobic effect is related to the introduction of a hydrocarbon into water which results in a structural rearrangement with increased order of the water close to the solute. Thus, the overall result of the host-guest combination depends on the negative contribution to entropy due to the association of the host and the guest molecules and the corresponding restriction of freedom degrees, in particular those of the guest molecule which impacts the enthalpy contribution, and a positive contribution due to the release of water from the cavity.

Given the differences in chemical structures of every hydrochloride anaesthetic, the differences in the proportion by which the binding entropy and enthalpy contribute to the Gibbs energy reflect the differences in the interaction established with β-CD [36-38].

As mentioned above, the value of Q can be calculated (for any designated values of n, K, and ΔH) at the end of the ith injection but the correct fitting process deals with the heat released from the ith injection, ΔQ(i), which is given by the following expression.

$$\Delta Q(i) = Q(i) + \frac{dV_i}{V_0}\left[\frac{Q(i) + Q(i-1)}{2}\right] - Q(i-1)$$

The process of fitting experimental data then involves 1) initial guesses of n, K, and ΔH; 2) calculation of ΔQ(i) for each injection and comparison of these values with the measured heat for the corresponding experimental injection; 3) improvement in the initial values of n, K, and ΔH and 4) iteration of the above procedure until no further significant improvement in fit occurs with continued iteration.

From the n values on **Table 2**, it is clear that TC,HCl complexation fits perfectly with the 1:1 model with the best complexation constant value in agreement with UV-Visible deduction. The corresponding process is almost equally controlled by enthalpy and entropy

contributions compared to PC,HCl that appears to be more dependent on entropy variation.

Table 2 Thermodynamic parameters ΔH, TΔS, ΔG and equilibrium constants K for complexation between LAs and β-CD at 298.15 K.

Guest	n	K (M^{-1})	ΔH (kJ/mol)	TΔS (kJ/mol)	ΔG (kJ/mol)
TC	0.1	174	-	-	-
TC, HCl	0.992	485	−6.64	8.69	−15.33
PC, HCl	1.545	390	−4.371	10.42	−14.79

Solid inclusion complex studies

In order to accomplish a comprehensive study, DSC and FT-IR methods were used for a rapid qualitative investigation by comparing the behavior of single components and their inclusion compounds.

Thermal analysis (DSC)

The DSC curves of solid state pure components and of inclusion complex between LA drugs and β-CD are shown in **Figure 5**. The DSC profiles of the pure components (tetracaine, β-CD) and their corresponding binary systems (physical mixtures and kneading sample) are shown in **Figure 5(a)**.

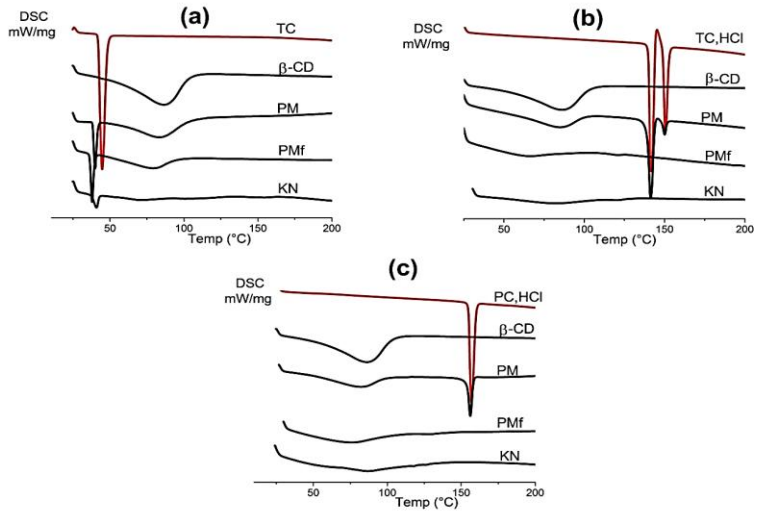

Figure 5 DSC curves of βCD, LAs, physical mixture (PM), physical mixture with grinding (PMf) kneaded (KN) products. (a): Basic tetracaine, (b): Tetracaine hydrochloride, and (c): Procaine hydrochloride).

The thermogram of pure β-CD shows a multi-stage dehydration process from 35 to 137 °C. The 1st stage of water elimination appeared as a wide endothermic band, below 100 °C (centered around 86 °C), which corresponds to the release of weak bound surface water molecules [39,40]. The thermal curve of TC sample presents a single endothermic signal with an onset peak at 42.12 °C and a maximum at 44.8 °C, corresponding to the melting point of the TC. The thermal curve of the physical mixture obtained with hard grinding noted PM_f seems to be the same as PM sample obtained due to the superposition of the 2 pure components curves, except the melting peak maximum which slightly shifts to 42 °C underlying the effect of grinding process which may modify the structural parameters of the TC crystal. The thermal curve of the solid inclusion complex of TC with β-CD obtained by kneading method showed a significant decrease in the intensity of the TC endothermic peak at 44.8 °C (**Figure 5(a)**). The incomplete disappearance of the crystalline melting peak of TC in the DSC curve can be assumed as an evidence of the weak insertion of the TC molecule inside the β-CD cavity. **Figure 5(b)** shows 2 sharp endothermic peaks at 139.7 and 149.52 °C which

are indicative of the presence of 2 crystalline species as already demonstrated by Giron *et al.* [41].

When the TC, HCl is mixed with β-CD without hard grinding the obtained physical mixture PM shows the presence of the earlier 2 peaks of TC, HCl with a signal attenuation of the 149 °C peak revealing its instability (switching to the 139.7 °C specie) or that this specie is hypothetically incorporated spontaneously into β-CD. The thermograms of TC, HCl/β-CD inclusion complex prepared by physical mixing PM, by grinding PM_f or by kneading KN (1:1) show complete disappearance of the endothermic peaks characteristic of TC, HCl and the shift of the broad β-CD water peak due to the dehydration process. These sign the successful inclusion complex formation and changes in hydration dynamics (The drug is no longer in its free crystalline form and the high-energy water molecules are expelled from the cavity od the CD). **Figure 5(c)** shows that the characteristic thermal profile of the drug (PC, HCl) is close to the thermal profile observed with TC, HCl except the presence of a unique melting peak at 153 °C. When the corresponding physical mixture PM enthalpogram is compared to the enthalpograms of the pure host or guest molecules, it easy to note the perfect superposition without peak shift. When the PM_f and kneading (KN) samples are compared to the pure samples the melting peak of the drug disappears completely with a weak trace of the water signal in contrast of TC, HCl case. For PC, HCl and TC, HCl mixtures it is evident that the complexation takes place for both kneading and PM_f samples. This agrees with the results deduced from UV-Visible and ITC experiments.

Fourier transform infrared spectroscopy (FT-IR)

The FT-IR spectroscopy technique was used for qualitative investigation of the interaction of LA and β-CD. **Figure 6** shows the FT-IR spectra of LA, β-CD and their 1:1 inclusion complexes, in the solid state. The FT-IR spectra of pure β-CD and the corresponding LA are presented at the top of each spectral series of spectra and correspond to the published spectra in literature [42].

The confirmation of the inclusion process between the guest and host molecules using FT-IR spectroscopy is based on the concept that after inclusion into the CD cavity the freedom of some bonds will be restricted due to the non-covalent interaction such as hydrophobic interactions, Van der Waals interactions and hydrogen bonding between the interacting molecules. This is expected to influence the peak intensities of the corresponding frequencies. This approach is the common method recommended in this kind of interaction and compares well with approaches used in studies dealing with the synthesis of doped-nanoparticles where bonds are cleaved and others are formed when exogenous material are entrapped into the native nanoparticle's structure [43]. Furthermore, the preparation of the physical mixture PM is a good method to estimate the inclusion phenomena, so the comparison becomes more valuable.

As shown in (**Figure 6**) and according to the corresponding chemical structure, the characteristic peaks of β-CD appear respectively at 3,300, 2,900 and 1,630 cm^{-1} for O-H, C-H and C=O bonds stretching as reported by Abou-Okeil *et al.* [42]. Additionally, other peaks are prominent at 1,419 and at 1,335 cm^{-1} for C-H bond wagging and bending respectively while the distinctive signal at 1,020 cm^{-1} is attributed to the C-O bond stretching.

For the LA molecules studied in this work, they share almost a wide range of the IR spectrum since they all contain the same para-amino-acetate benzene group. In the case of hydrochloride molecules, the differences are related to the butyl chain between tetracaine and procaine as well as their corresponding amino groups. In the case of basic tetracaine and its corresponding acidic conjugate TC, HCl the differences may arise from the subtle conformational distinction between the amine and the amino groups.

The comparison of TC, HCl and TC spectra showed that almost the same signals are observed with little shift in peaks positions. Indeed, for TC, HCl and TC molecules N-H symmetric stretching is observed at 3,371 cm^{-1} and the CH stretching vibrations appear at 2,947 and 2,865 cm^{-1} for TC, HCl and at 2,952 and 2,861 cm^{-1} for TC. At 1,672 cm^{-1} one identifies C=O stretching for TC, HCl which shifts to 1,683cm^{-1} in the case of TC. The aromatic ring vibration modes are situated at 1,600 for TC but observed at 1,500 cm^{-1} for TC, HCl.

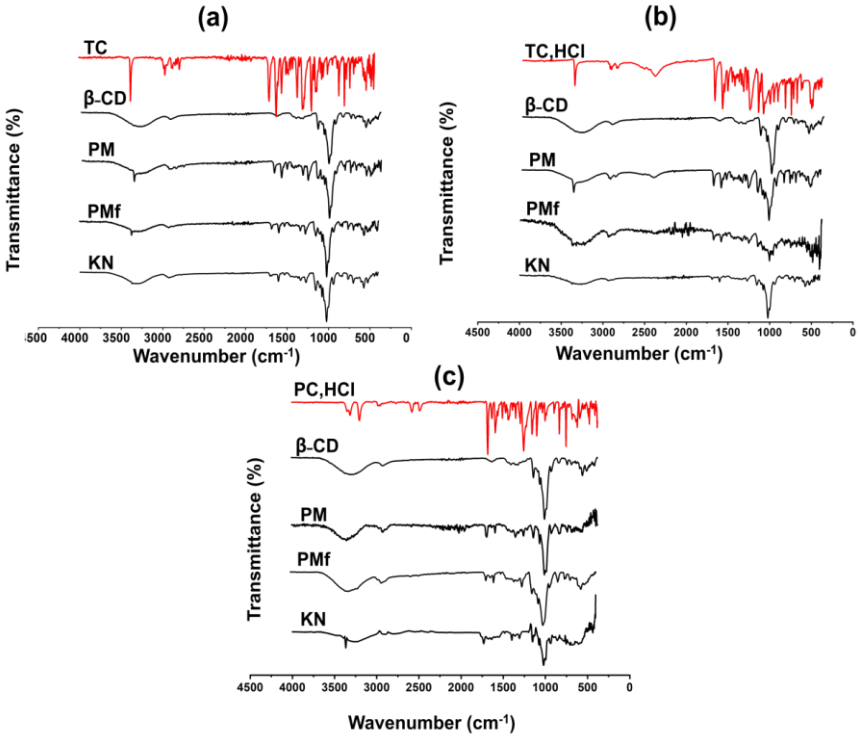

Figure 6 FT-IR spectra of βCD, LAs, physical mixture (PM), physical mixture with grinding (PMf) kneaded (KN) products. (a): Basic tetracaine, (b): Tetracaine hydrochloride, and (c): Procaine hydrochloride).

The FT-IR spectrum of the TC/β-CD (**Figure 6(a)**) showed some significant changes when related to pure TC spectrum. The FT-IR spectrum of the TC/β-CD complex showed the same distinctive bands with reduced peak intensities compared to pure TC spectrum. The N-H symmetric stretching signal at 3,371 cm^{-1} is dramatically reduced in the inclusion complexes (KN) spectrum. This is because the para-amino-acetate benzene group of the drug is probably entrapped into the β-CD cavity which hinders its vibration mode. As a result of inclusion complex formation, the broad O-H signal of pure β-CD at 3,300 cm^{-1} was narrowed in the FT-IR spectrum of the inclusion complexes. This constitutes a good indication of the formation of the inclusion complex [44].

The FT-IR spectrum of the TC, HCl/β-CD showed some significant changes compared to pure TC, HCl spectrum. The FT-IR spectrum of the TC, HCl/β-CD complex showed the same distinctive bands but with more attenuated intensities compared to pure TC, HCl spectrum. The N-H symmetric stretching at 3,376 cm^{-1} completely disappeared in the KN inclusion complex revealing that the N-H bond experiences shielding from the β-CD hydrophobic interior, altering its dipole moment and IR activity.

For PC, HCl/ β-CD (**Figure 6(c)**), the same observations are noted where a decrease in the intensity of several peaks occurs. We can mention that the intensity of 1,695 cm^{-1} peaks of the drug (Conjugated C=O stretching mode) that decreases as well as the peaks at 848 and 769 cm^{-1} which are almost unrecognizable. The N-H symmetric stretching at 3,370 cm^{-1} completely disappeared for the PM and PM_f samples but still present for the KN one. In the case of TC and TC, HCl samples this peak disappears completely for KN samples but still present in PM and PM_f samples. This is the opposite behavior noticed for PC, HCl complexes. From these observations, we suggest that in the case of TC and TC, HCl molecules the inclusion into the CD cavity occurs with the tertiary amine group instead of the expected hydrophobic butyl chain and in the case of PC, HCl, the inclusion occurs from the primary amine side instead of its tertiary amino group. This suggestion is based on the fact that the kneading method reveals that the contribution of the added water during the PC, HCl complex preparation is less marked whereas it is crucial for the inclusion process in the case of TC or TC, HCl

samples.

Conclusions

This study examined the complexation of three anesthetic drugs with β-cyclodextrin (β-CD) in both liquid and solid states using various techniques, including UV-Visible spectrophotometry, isothermal calorimetry, differential scanning calorimetry, and infrared spectrometry. The UV-Visible results indicated the formation of drug/β-CD complexes in a 1:1 stoichiometric ratio, as evidenced by the presence of isobestic points and hyperchromic and bathochromic shifts in the UV spectra. Among the complexes, the TC, HCl complex exhibited the highest stability, reflected by its significant complexation constant (K11 = 403.27). The thermodynamic analysis conducted in the liquid state through isothermal titration calorimetry (ITC) corroborated the UV-Visible findings, demonstrating that complexation is thermodynamically favorable for both TC, HCl/β-CD and PC, HCl/β-CD (with K values of 485 M-1 for TC, HCl and 390 M-1 for PC, HCl). However, the formation of the TC/β-CD complex was not satisfactorily confirmed, as indicated by an irregular enthalpogram. Furthermore, the process was determined to be driven by entropy, with a moderate contribution from enthalpy. In the solid state, the formation of host-guest complexes was qualitatively validated using differential scanning calorimetry (DSC) and Fourier-transform infrared (FT-IR) spectroscopy. The DSC results indicated that the hydrochloride drug-cyclodextrin complexes could be readily formed through well grinded physical mixing or kneading preparations, suggesting a favorable outcome from a pharmaceutical perspective. Conversely, the IR analysis revealed that the hydrophobic hydrocarbon chain of the drug does not necessarily need to be the primary component enclosed within the CD cavity.

Acknowledgements

The authors would like to thank the DGRSDT, Algeria and University of Mascara for their technical and financial supports.

References

[1] H Fozzard, P Lee and G Lipkind. Mechanism of local anesthetic drug action on voltage-gated Sodium channels. *Current Pharmaceutical Design* 2005; **11(21)**, 2671-2686.

[2] S Hannongbua, W Treesuwan and W Boonyarat. *Advanced molecular modeling techniques applied to ion channels and their inhibitors*. *In*: SP Gupta (Ed.). Ion channels their inhib. Springer Berlin, Heidelberg, Germany, 2011, p. 53-78.

[3] SA Fernandes, LF Cabeça, AJ Marsaioli and ED Paula. Investigation of tetracaine complexation with beta-cyclodextrins and p-sulphonic acid calix arenes by nOe and PGSE NMR. *Journal of Inclusion Phenomena and Macrocyclic Chemistry* 2007; **57**, 395-401.

[4] BJ Drakulić, C Zalaru and M Iovu. Acutetoxicity of substituted 2-(*1H*-pyrazol-1-yl) acetanilides and related commercially available local anesthetics toward mice. A grind/almond-based 3-D QSAR study. *QSAR & Combinatorial Science* 2009; **28(2)**, 206-217.

[5] N Kaboudi, SG Asl, N Nourani and A Shayanfar. Solubilization of drugs using beta-cyclodextrin: Experimental data and modeling. *Annales Pharmaceutiques Françaises* 2024; **82(4)**, 663-672.

[6] OE Nicolaescu, I Belu, AG Mocanu VC, Manda, G Rău, AS Pîrvu, C Ionescu F, Ciulu-Costinescu, M Popescu and MV Ciocîlteu. Cyclodextrins: Enhancing drug delivery, solubility and bioavailability for modern therapeutics. *Pharmaceutics* 2025; **17(3)**, 288.

[7] GA Gonzalez, C Betbeze, R Wills, A Eddy, C Mochal-King and RL Fontenot. Effects of subconjunctival ropivacaine, liposomal bupivacaine, and mepivacaine on corneal sensitivity in healthy horses. *Veterinary Surgery* 2023; **52(7)**, 1041-1049.

[8] TA Bauer, NK Horvat, O Marques and S Chocarro, C Mertens, S Colucci, S Schmitt, LM Carrella, S Morsbach, K Koynov, F Fenaroli, P Blümler, M Jung, R Sotillo, MW Hentze, MU Muckenthaler and M Barz. Core cross-linked polymeric micelles for specific iron delivery: Inducing sterile inflammation in macrophages. *Advanced Healthcare Materials* 2021; **10(19)**, 2100385.

[9] N Azum, MM Alotaibi, M Ali, MA Rub, HM Marwani, KA Alamry and AM Asiri.

Investigation of an anaesthetic drug (tetracaine hydrochloride) in the presence of ionic fluid and surfactant: Mixed micellization & spectroscopic studies. *Journal of Molecular Liquids* 2023; **370**, 121057.

[10] C Kappel, C Seidl, C Medina-Montano, M Schinnerer, I Alberg, C Leps, J Sohl, AK Hartmann, M Fichter, M Kuske, J Schunke, G Kuhn, I Tubbe, D Paßlick, D Hobernik, R Bent, K Haas, E Montermann, K Walzer, M Diken, …, and S Grabbe. Density of conjugated antibody determines the extent of Fc receptor dependent capture of nanoparticles by liver sinusoidal endothelial cells. *ACS Nano* 2021; **15(9)**, 15191-15209.

[11] RAFD Lima, MBD Jesus, S Cereda, CM Tofoli, GR Cabeça, LF Mazzaro and E Paula. Improvement of tetracaine antinociceptive effect by inclusion in cyclodextrins. *Journal of Drug Targeting* 2012; **20(1)**, 85-96.

[12] RS Teixeira, FJ Veiga, RS Oliveira, SA Jones, SM Silva, RA Carvalhoand and AJ Valente. Effect of cyclodextrins and pH on the permeation of tetracaine: Supramolecular assemblies and release behavior. *International Journal of Pharmaceutics* 2014; **466(1-2)**, 349-358.

[13] W Sansanayudh, T Phansucharitthai and Sansanayudh. The effect of cold tetracaine on the severity of burning sensation upon instillation. *Clinical Ophthalmology* 2018; **12**, 2377-2382.

[14] T Ayuse, S Kurata and T Ayuse. Successful dental treatments using procaine hydrochloride in a patient afraid of local anesthesia but consenting for allergic testing with lidocaine: A case report. *Local and Regional Anesthesia* 2020; **13**, 99-103.

[15] SA Zahavi, Y Ouanounou, PL Carlen and A Ouanounou. Local anaesthetic-induced seizures: A review. *Frontiers of Oral and Maxillofacial Medicine* 2025; **7**, 1-8.

[16] PB Dias, MD AR Parchen and D Wasilewski. Comparison of proparacaine, tetracaine, and oxybuprocaine in corneal sensitivity measurement. *Journal of Ocular Pharmacology and Therapeutics* 2024; **40(4)**, 215-221.

[17] AH Jeske. *Local anesthetics*. *In*: AH Jeske (Ed.). Contemporary dental pharmacology. Springer Cham, Germany, 2024, p. 9-23.

[18] W Rosenkrantz. Practical applications of topical therapy for allergic, infectious, and seborrheic disorders. *Clinical Techniques in Small Animal Practice* 2006; **21(3)**, 106-116.

[19] H Faghihi, SM Rajaei, H Ostadhasan and HE Alagha. Effect of topical 0.5 % tetracaine hydrochloride on intraocular pressure in ophthalmologically normal cats. *Journal of Feline Medicine and Surgery* 2022; **24(2)**,185-188.

[20] C Margeti, C Kostakis, V Tsioli, K Karagianni and E Flouraki. Local anaesthesia techniques in dogs and cats: A review study. *Pets* 2024; **1(2)**, 88-119.

[21] T Kovacs, P Nagy, G Panyi, L Szente, Z Varga and F Zakany. Cyclodextrins: Only pharmaceutical excipients or full-fledged drug candidates? *Pharmaceutics* 2022; **14(12)**, 2559.

[22] B Ramos-Martínez, C Dávila-Pousa, V Merino-Bohórquez, M García-Palomo and MP Flox-Benítez. Use of cyclodextrins as excipients in pharmaceutical products: why not in extemporaneous preparations? *Farmacia Hospitalaria* 2022; **46(1)**, 31-39.

[23] G Kali, S Haddadzadegan and AB Schnürch. Cyclodextrins and derivatives in drug delivery: New developments, relevant clinical trials, and advanced products. *Carbohydrate Polymers* 2023; **324(1)**, 121500.

[24] H Liu, S Guo, S Wei, J Liu and B Tian. Pharmacokinetics and pharmacodynamics of cyclodextrin-based oral drug delivery formulations for disease therapy. *Carbohydrate Polymers* 2023; **329**, 121763.

[25] JY Liu, X Zhang and T Bıngren. Selective modifications at the different positions of cyclodextrins: A review of strategies. *Turkish Journal of Chemistry* 2020; **44(2)**, 261-278.

[26] A Haroun, A Osman, S Ahmed and AH Elghandour. Synthesis and characterization of ibuprofen delivery system based on β - cyclodextrin. *Trends in Science* 2022; **19(19)**, 5825.

[27] CM Santamaria, A Woodruff, R Yang and DS Kohane. Drug delivery systems for prolonged duration local anesthesia. *Materials Today* 2017; **20(1)**, 22-31.

[28] KVB Pharm, MRB Pharm and MM Patel. Insight on nano drug delivery systems with targeted therapy in treatment of oral cancer. *Nanomedicine: Nanotechnology, Biology and Medicine* 2023; **49(9)**, 102662.

[29] S Prabu, K Sivakumar, SK Nayaki and R Rajamohan. Host-guest interaction of cytidine in β -cyclodextrin microcavity: Characterization and docking study. *Journal of Molecular Liquids* 2016; **219**, 967-974.

[30] C Merino, E Junquera, J Jime and E Aicart. Effect of the presence of cyclodextrin on the solution behavior of procaine hydrochloride spectroscopic and thermodynamic studies. *Langmuir* 2000; **16(14)**, 1557-1565.

[31] P Fini, M Castagnolo, L Catucci, P Cosmaa and A Agostiano. Inclusion complexes of rose bengal and cyclodextrins. *Thermochimica Acta* 2004; **418(1-2)**, 33-38.

[32] H Boudjoras, T Fergoug, M Azayaz, Y Bouhadda, NM Araibi and C Zelmat. Temperature effect on the encapsulation of the drug tetracaine hydrochloride in different cyclodextrins. *Malaysian Journal of Analytical Sciences* 2022; **26(1)**, 164-175.

[33] BN Nalluri, KPR Chowdary, RV Kolapalli, AR Hayman and G Becket. Physicochemical characterization and dissolution properties of nimesulide-cyclodextrin binary systems. *AAPS PharmSciTech* 2003; **4(1)**, E2.

[34] GA Holdgate and WHJ Ward. Measurements of binding thermodynamics in drug discovery. *Drug Discovery Today* 2005; **10(22)**, 1543-1550.

[35] D Jakšić, MŠ Klarić, H Rimac, R Kerep and I Piantanida. Cyclodextrin-based displacement strategy of sterigmatocystin from serum albumin as a novel approach for acute poisoning detoxification. *International Journal of Molecular Sciences* 2023; **24(5)**, 4485.

[36] H Li, X Xu, M Liu, D Sun and L Li. Microcalorimetric and spectrographic studies on host-guest interactions of α-, β-, γ- And Mβ-cyclodextrin with resveratrol. *Thermochimica Acta* 2010; **510(1-2)**, 168-172.

[37] K Bouchemal and S Mazzaferro. How to conduct and interpret ITC experiments accurately for cyclodextrin-guest interactions. *Drug Discovery Today* 2012; **17(11-12)**, 623-629.

[38] A Pîrnău, M Mic, M Bogdan and I Turcu. Characterization of β-cyclodextrin inclusion complex with procaine hydrochloride by 1H NMR and ITC. *Journal of Inclusion Phenomena and Macrocyclic Chemistry* 2014; **79**, 283-289.

[39] MM Doile, KA Fortunato, IC Schmücker, SK Schucko, MAS Silva and PO Rodrigues. Silva and PO Rodrigues. Physicochemical properties and dissolution studies of dexamethasone acetate-β-cyclodextin inclusion complexes produced by different methods. *AAPS PharmSciTech* 2008; **9(1)**, 314-321.

[40] U Gala, MC Chuong, R Varanasi and H Chauhan. Characterization and comparison of lidocaine-tetracaine and lidocaine-camphor eutectic mixtures based on their crystallization and hydrogen-bonding abilities. *AAPS PharmSciTech* 2015; **16(3)**, 528-536.

[41] D Giron, M Draghi, C Goldbronn, S Pfeffer and P Piechon. Study of the polymorphic behaviour of some local anesthetic drugs. *Journal of Thermal Analysis* 1997; **49(2)**, 913-927.

[42] A Abou-Okeil, M Rehan, SM El-Sawy, MK El-bisi, OA Ahmed-Farid and FA Abdel-Mohdy. Lidocaine/β-cyclodextrin inclusion complex as drug delivery system. *European Polymer Journal* 2018; **108**, 304-310.

[43] KO Eshchanov and MM Baltaeva. Study of the interaction of sorbed silver, gold and copper ions with functional groups on hydrolyzed fibroin using Charmm 22 force field calculations. *Chemical Review & Letter* 2022; **5**, 161-168.

[44] NY Rahim, FH Samad, AM Rohisham. Spectroscopic studies of inclusion complex glipizide and β -cyclodextrin. *Malaysian Journal of Analytical Sciences* 2019; **23(5)**, 789-798.